SUPPLEMENTAL FIGURE LEGENDS

Figure S1. BMI1 expression is elevated in metastatic human samples and cell lines. Related to Figure 1.

(A) Box and whisker plots (5-95 percentile) show BMI1 expression in metastatic versus primary melanoma samples (GSE46517 dataset) and in samples derived from melanoma mouse models with or without metastatic capacity (GSE29074 dataset). (B) BMI1 mRNA levels in human melanoma cell lines derived from primary tumors or metastatic sites. (C) Western blotting showing BMI1 levels, with HSP90 as a loading control, in the B16F0, B16F1 and B16F10 cells. (D) Western blotting showing GFP and BMI1 levels, with HSP90 as a loading control, in our MA2, B16F0, B16F1, A375 and S91 variants. (E) Western blotting showing BMI1 levels, with HSP90 as a loading control, in all our BMI1-overexpressing variants. UACC-62 and SK-Mel-2 cell lines were used as reference for BMI1 expression. Values below the corresponding lanes show BMI1 fold change between BMI1 and CTL variants or . SK-Mel-2 and UACC-62. (F) Representative images of H&E staining of lungs after tail vein injections with CTL or BMI1 B16F10 cells showing lung tumors.

Figure S2. BMI1 high expression enhances metastatic potential of melanoma cells. Related to Figure 2.

(A) Representative images of wound healing assays with CLT or BMI1 B16F10 cells. (B) Transwell migration assays with CTL and BMI1 variants of A375, B16F10 and S91 cells. Representative images and quantifications are shown. (C) Murine lung sections 48 hours post injection of CMRA-labelled parental or BMI1 B16F10 cells (red) were stained with CD31 antibody (green) to visualize blood vessels and counter-stained with DAPI (blue). Bar graph show quantification of extravasated melanona cells in 3 lungs per cell type. (D) Adhesion on collagen (left panel) and fibronectin (right panel) of CTL and BMI1 MA2 cells. At the indicated time, cells were fixed, stained with crystal violet and O.D. was measured.

Representative images and quantification at 15 and 30 minutes are shown. (E) Morphological changes in CTL and BMI1 A375 (left) and MA2 (right) cells; representative images are shown. The box plots (min to max) show the quantification of cell morphology expressed as shape factor ($4\pi A/P^2$). Perimeters of 180 cells were determined. (F) Gelatin zymography performed on culture media from CTL and BMI1 A375 (top panel) and MA2 (bottom panel) cells shows activity of MMP2. (G) Low seeding assay with CTL and BMI1 A375 (left) or MA2 (centre) and B16F0 (right)cells. 500 cells were seeded and cultured for 10 days. Cells were then fixed, stained with crystal violet and the colonies were counted. Representative images and quantification are shown.

Figure S3. BMI1 expression does not alter PTEN-AKT signaling. Related to Figure 3.
Western blot analysis looking at PTEN and AKT pathways in CTL and BMI1 A375 cells not starved or serum starved for 48 or 72 hours (A-B), CTL and BMI1 MA2 cells (B), CTL and BMI1 B16F10 cells (C), CTL and BMI1 MA2 cells serum starved for 18 hours and then stimulated with 10% serum for 10 and 30 minutes (D). Analysis of β-catenin and PTEN pathways on CTL and BMI1 B16F10 (E), A375 (F,H) and MA2 cells (G,I).

Figure S4. Invasive signature induced by BMI1 expression. Related to Figure 3.
(A) The differentially expressed (DE) gene list was analyzed with IPA (Ingenuity Pathway Analysis) for functional analysis. The Graph shows the canonical pathways that are significantly altered. The x-axis shows the significance (value of -log (p)). Pathways are listed from most significant to least and the black vertical line represents the cutoff for significance (p-value of 0.05). (B) Gene Set Enrichment Analysis (GSEA) performed with the RNA-Seq dataset identified enriched signatures of extracellular matrix components, acquired resistance to therapy, EMT, and cancer progression. ES, enrichment score; FDR, false discovery rate. (C) Heat maps of specific pathways found to be activated in the BMI1 data set.

Figure S5. **Signaling pathway alteration and drug resistance phenotype in BMI1 overexpressing cells. Related to figure 4 and 5.**

(A-B) qPCR analysis on total RNA from B16F10-BMI1 overexpressing (A) and B16F10 cells upon BMI1 knockdown (B), confirming the differential expression of representative genes involved in EMT, TGFβ, non-canonical Wnt/PKC and EGF/PDGF pathways. Results shown are mean ± s.d. In B statistical significance was calculated with Two Way Anova and Tukey's multiple comparisons test. * indicates significance versus B16F10 sh-CTL. (C) Analysis of PKC pathway in CTL and BMI1 A375 cells. (D) Analysis of SMAD2-3 and Fibronectin expression levels in CTL and BMI1 A375 and MA2 cells. (E) Analysis of Snail expression in MA2 variants upon BMI1 overexpression or knockdown.(F) Analysis of EGFR and cJun expression on CTL and BMI1 MA2 cells treated or not treated with BRAF inhibitor PLX4720. For all western blot panels HSP90 was used as loading control. (G) CTL and BMI1 MA2 cells were subjected to treatment with different chemotherapeutic agents for 48 hours and cell death percentage was evaluated by APC-Annexin V staining and FACS analyses. Treatment with PLX4720 was used as control for resistance. (H) MA2 cells carrying sh-Ctl or BMI1 shRNAs, Sh1 or Sh2, were assessed for response to treatment with PLX4720 by analysis of growth inhibition after 18 days. Representative images are shown. (I) Wound healing migration assay with CTL and BMI1 MA2 cells either non resistant to PLX4720 (left bars), resistant to PLX4720 (selected by exposure to 2μM PLX4720) and maintained in media without drug (middle bars), or resistant to PLX4720 and maintained in media with drug (right bars). (J) qPCR analysis on total RNA from MA2-shCTL cells and MA2-BMI1 with (sh-2) or without (sh-Ctl) Wnt5a knockdown. In J statistical significance was calculated with Two Way Anova and Tukey's multiple comparisons test. * indicates significance versus MA2 sh-CTL.

Figure S6. Characterization of melanomas arising upon perinatal 4-OHT treatment. Related to Figure 6.

(A) Genomic DNA was isolated from pigmented lesions on the skin of 4-OHT treated mice and PCR analysis was used to confirm *Bmi1* allele recombination (top panel) in the presence of Tyr CRE-ER (bottom panel). (B) Newborn pups were treated on post-natal day 2 and 4 with 4-OHT on the ventral skin. In about 3 weeks they developed pigmented lesion all over the body (visibly on the ears, mouth, paws and on the skin). In about 5 weeks all animals needed to be euthanized and the necroscopy revealed the presence of highly pigmented lymph nodes (red arrow).

Figure S7. BMI1 induced signature does not correlate with outcome in other tumor types. Related to Figure 7.

Patient outcome based on BMI1 signature correlation (top 10% versus the remaining 90%) using TCGA lung adenocarcinoma, breast invasive carcinona and colon adenocarcinoma sets. Log-rank p-value is shown.

Supplemental Table S1.

List of differentially expressed genes in CTL and BMI1 A375 variants. Corresponding expression levels, normalized expression and statistics are shown.

Supplemental Table S2. List of genes from our BMI1-induced signature that presented a FC≥2 between A+B versus C subclasses and were observed in at least 2 of the 3 cohorts. Gene name, number of common cohorts and direction are shown.

Supplemental Table S3.

List of primers used for qPCR.

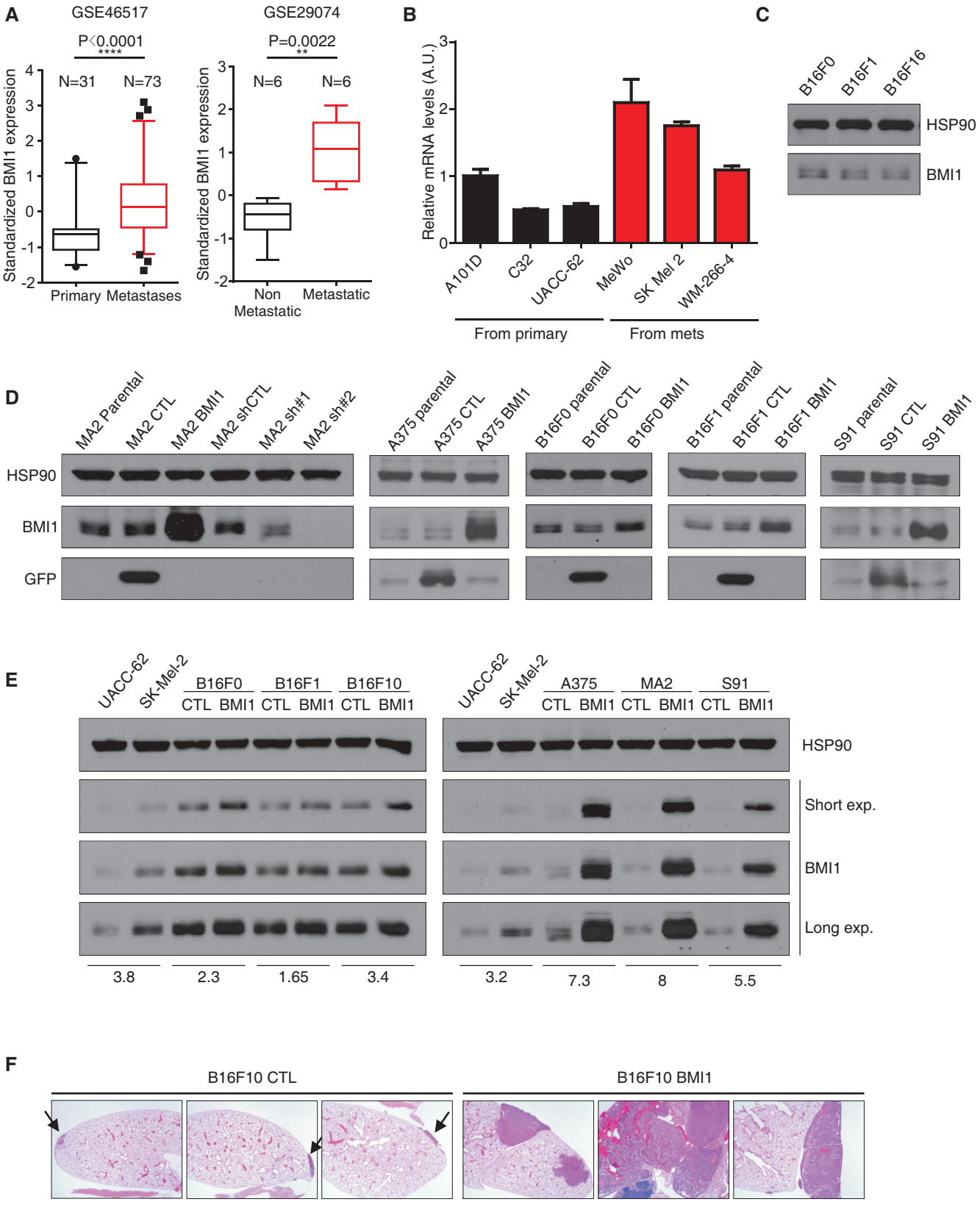
A
GSE46517
P<0.0001
****
N=31
N=73
Standardized BMI1 expression
Primary
Metastases
GSE29074
P=0.0022
**
N=6
N=6
Non Metastatic
Metastatic
B
Relative mRNA levels (A.U.)
A101D
C32
UACC-62
MeWo
SK Mel 2
WM-266-4
From primary
From mets
C
B16F0
B16F1
B16F16
HSP90
BMI1
D
MA2 Parental
MA2 CTL
MA2 BMI1
MA2 shCTL
MA2 sh#1
MA2 sh#2
A375 parental
A375 CTL
A375 BMI1
B16F0 parental
B16F0 CTL
B16F0 BMI1
B16F1 parental
B16F1 CTL
B16F1 BMI1
S91 parental
S91 CTL
S91 BMI1
HSP90
BMI1
GFP
E
UACC-62
SK-Mel-2
B16F0
B16F1
B16F10
CTL BMI1 CTL BMI1 CTL BMI1
A375
MA2
S91
HSP90
Short exp.
BMI1
Long exp.
3.8
2.3
1.65
3.4
3.2
7.3
8
5.5
F
B16F10 CTL
B16F10 BMI1

Ferretti_Supplemental Figure 2

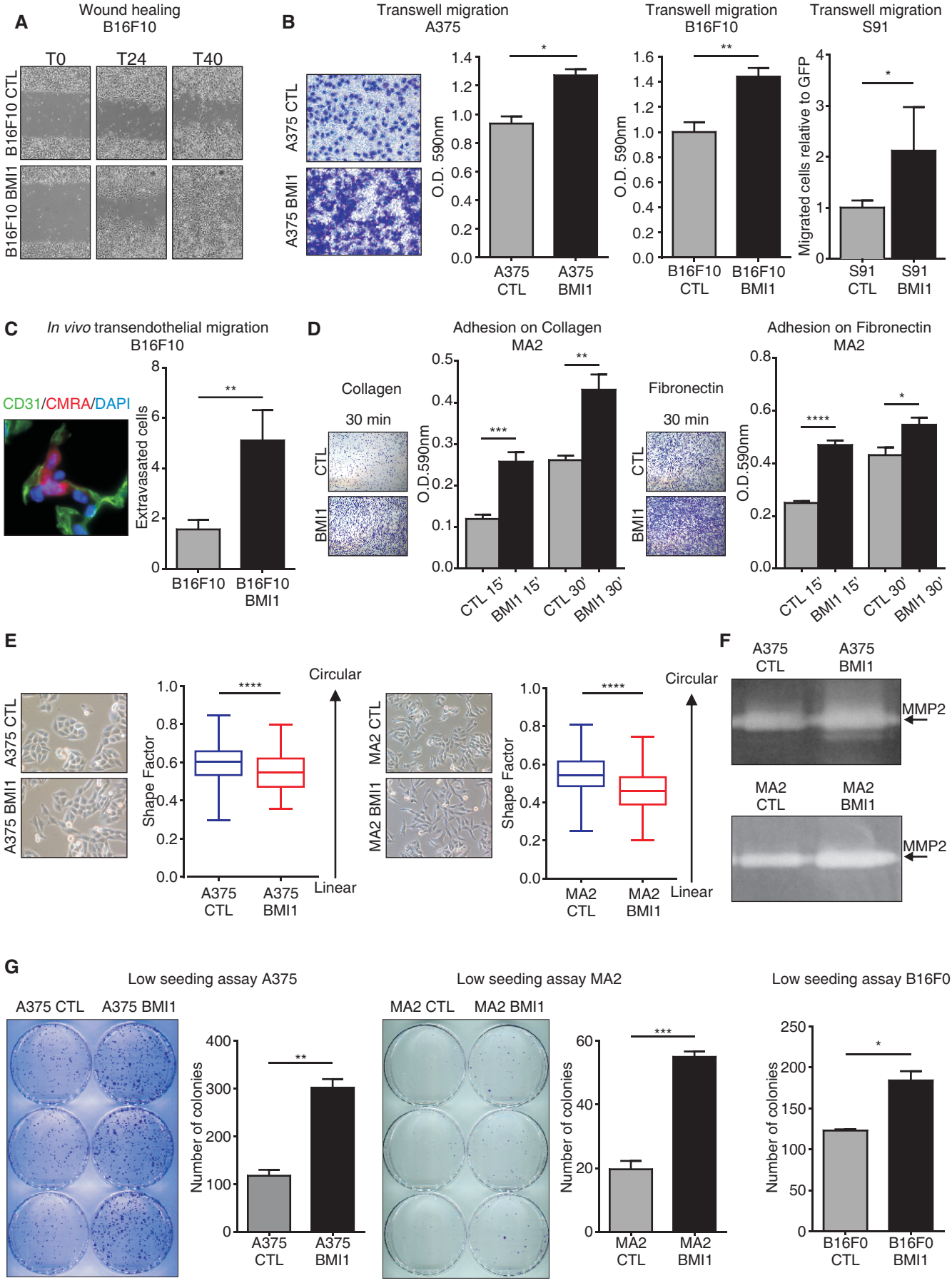

Ferretti_Supplemental Figure 3

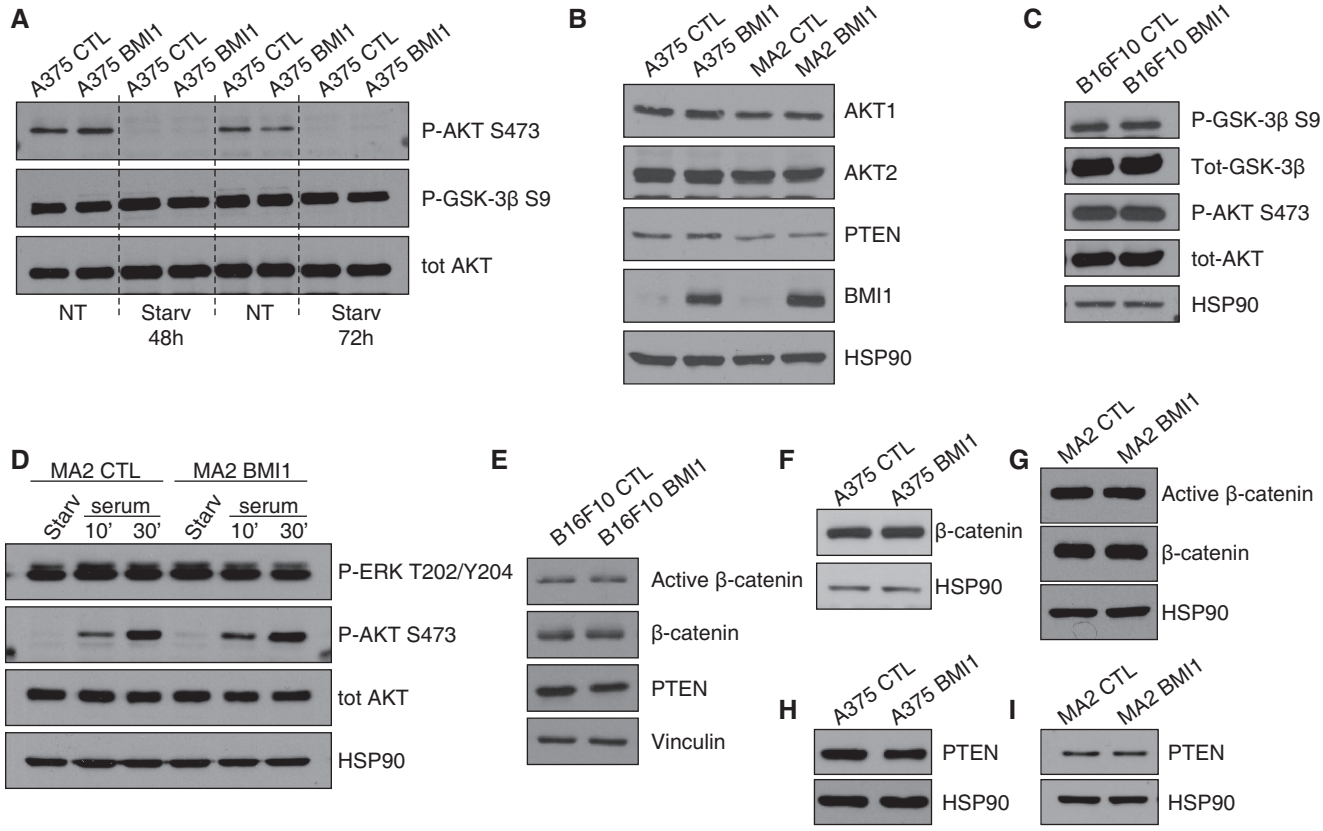

Ferretti_Supplemental Figure 4

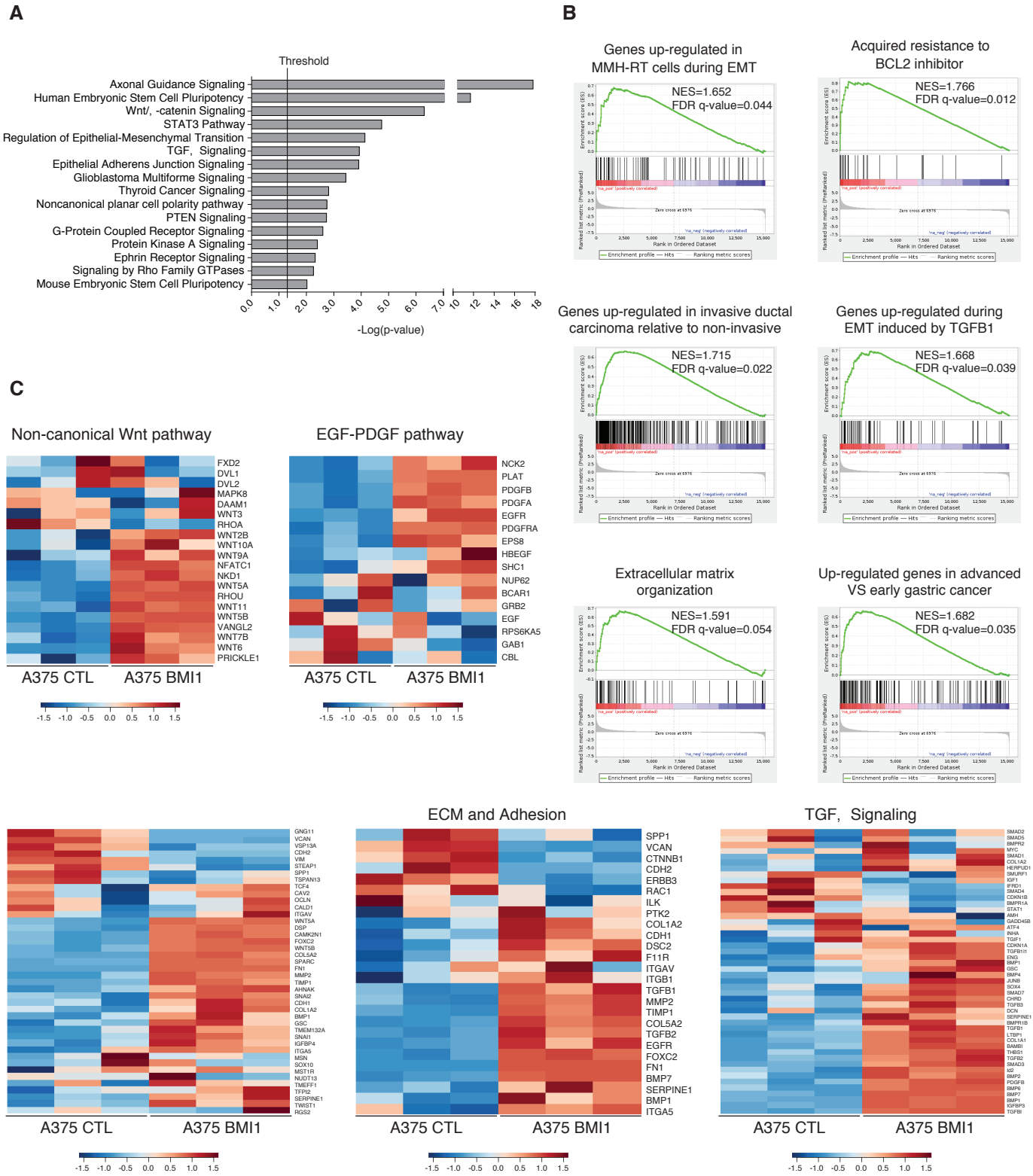

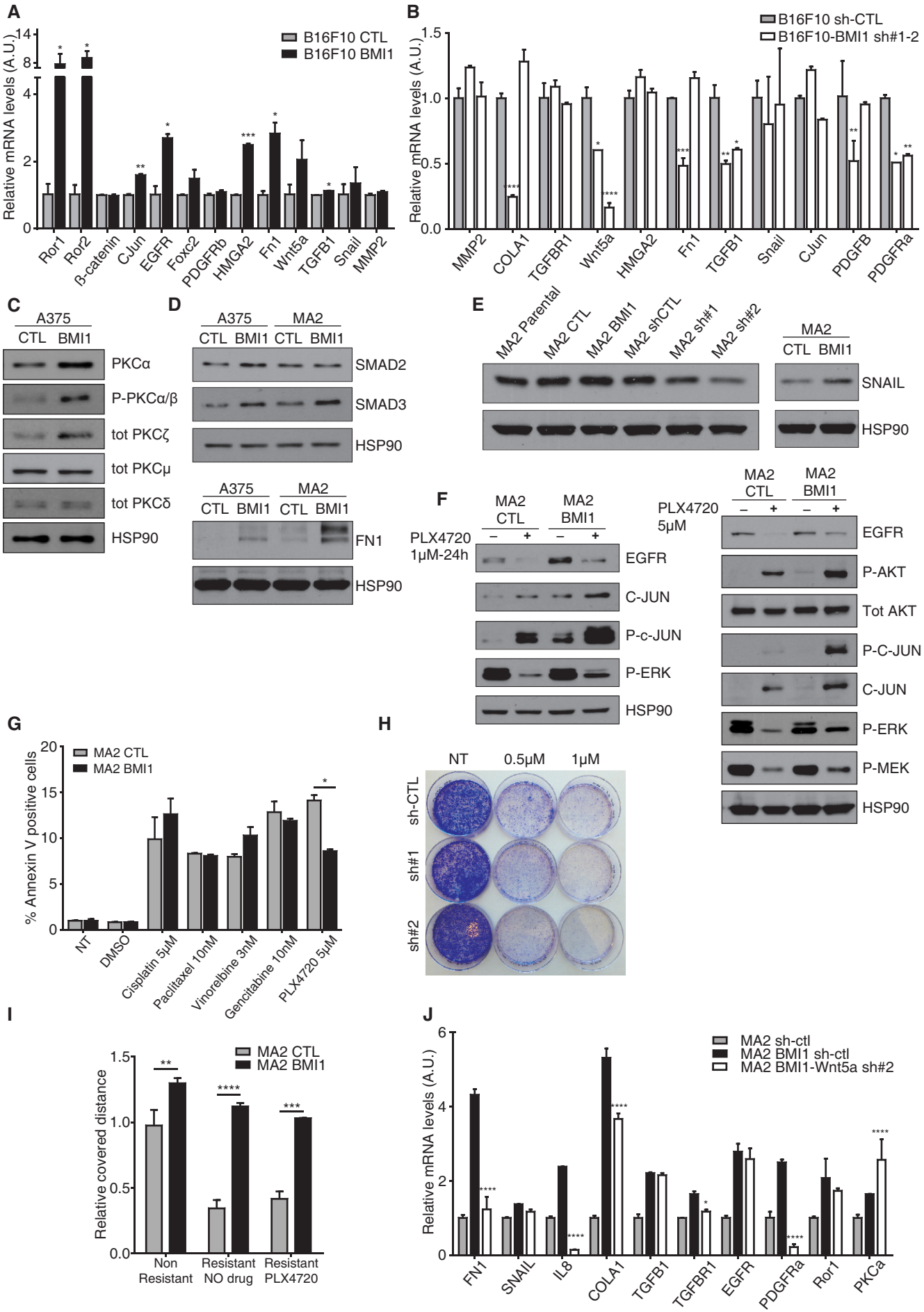
A
Relative mRNA levels (A.U.)
B16F10 CTL
B16F10 BMI1
Ror1
Ror2
β-catenin
CJun
EGFR
Foxc2
PDGFRb
HMGA2
Fn1
Wnt5a
TGFB1
Snail
MMP2
B
B16F10 sh-CTL
B16F10-BMI1 sh#1-2
MMP2
COLA1
TGFBR1
Wnt5a
HMGA2
Fn1
TGFB1
Snail
CJun
PDGFB
PDGFRa
C
A375
CTL BMI1
PKCα
P-PKCα/β
tot PKCζ
tot PKCμ
tot PKCδ
HSP90
D
A375 MA2
CTL BMI1 CTL BMI1
SMAD2
SMAD3
HSP90
FN1
E
MA2 Parental
MA2 CTL
MA2 BMI1
MA2 shCTL
MA2 sh#1
MA2 sh#2
SNAIL
F
PLX4720 1μM-24h
PLX4720 5μM
EGFR
C-JUN
P-c-JUN
P-ERK
P-AKT
Tot AKT
P-MEK
G
% Annexin V positive cells
MA2 CTL
MA2 BMI1
NT
DMSO
Cisplatin 5μM
Paclitaxel 10nM
Vinorelbine 3nM
Gencitabine 10nM
PLX4720 5μM
H
NT
0.5μM
1μM
sh-CTL
sh#1
sh#2
I
Relative covered distance
Non Resistant
Resistant NO drug
Resistant PLX4720
J
MA2 sh-ctl
MA2 BMI1 sh-ctl
MA2 BMI1-Wnt5a sh#2
FN1
SNAIL
IL8
COLA1
TGFB1
TGFBR1
EGFR
PDGFRa
Ror1
PKCa

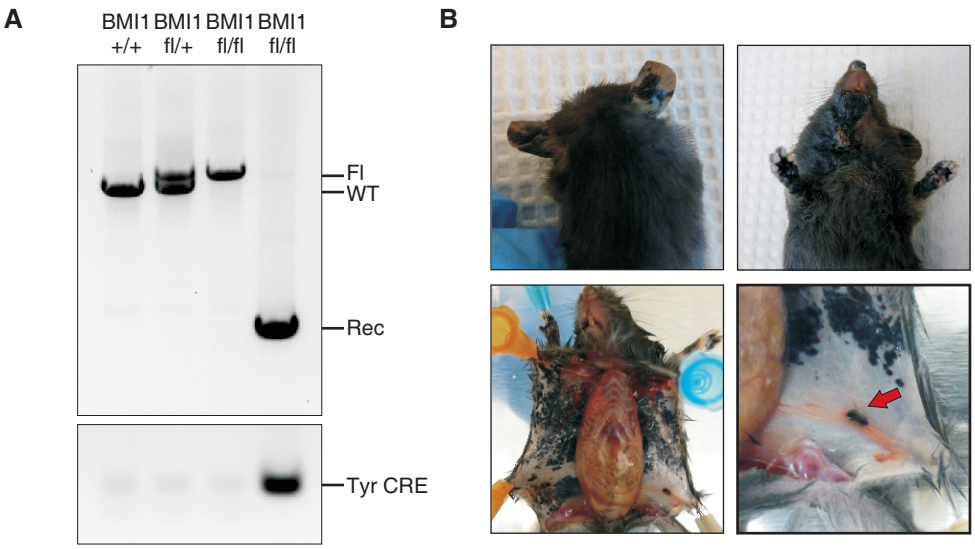
A
BMI1 +/+
BMI1 fl/+
BMI1 fl/fl
BMI1 fl/fl
Fl
WT
Rec
Tyr CRE
B

Ferretti_Supplemental Figure 7